

Excited-State Processes in Ruthenium(II) Bipyridine Complexes Containing Covalently Bound Arenes

Gerard J. Wilson,* Anton Launikonis, Wolfgang H. F. Sasse, and Albert W.-H. Mau

CSIRO, Division of Chemicals and Polymers, Private Bag 10, Rosebank MDC,
Clayton, Victoria 3169, Australia

Received: February 24, 1997; In Final Form: April 30, 1997[⊗]

The photophysical properties of a series of ruthenium trisbipyridine complexes covalently linked to aromatic chromophores of the type $[\text{Ru}(\text{bpy})_2(4\text{-methyl-4'-(2-arylethyl)-2,2'-bipyridine})]^{2+}(\text{ClO}_4)_2$, where aryl = 2-naphthyl ([Ru]-naphthalene), 1-pyrenyl ([Ru]-pyrene), and 9-anthryl ([Ru]-anthracene) have been investigated at room temperature and at 77 K. The photophysical properties of these bichromophores are determined by intramolecular energy-transfer processes that are governed by the relative positions of the various singlet and triplet energy levels. As a result, fluorescence from each of the pendant aromatic chromophores is completely quenched following their photoexcitation. For [Ru]-naphthalene the initial excitation energy is localized on the [Ru]-centered $^3\text{MLCT}$ state, whereas for [Ru]-anthracene the energy is localized on the anthracene triplet state. Since the [Ru]-centered $^3\text{MLCT}$ state and the lowest energy pyrene triplet state are isoenergetic, an equilibrium is established resulting in a long-lived room-temperature $^3\text{MLCT}$ emission from [Ru]-pyrene ($\tau = 5.23 \mu\text{s}$). At 77 K dual emission is observed from this bichromophore comprising pyrene phosphorescence and $^3\text{MLCT}$ emission, the relative proportions of which vary with time after the laser pulse.

1. Introduction

The $\text{Ru}(\text{bpy})_3^{2+}$ chromophore and its analogues are finding increasing use as components in multichromophore systems.¹ The generality and versatility of these chromophores have been highlighted by their use as (i) photosensitizers,² (ii) energy donors, relays, and acceptors,³ and (iii) electron donors, relays, and acceptors⁴ in many supramolecular systems. For such supramolecular systems to become truly useful supramolecular devices, it is necessary to both understand and control the flow of energy from the initially excited chromophore to the site where the energy is ultimately localized.

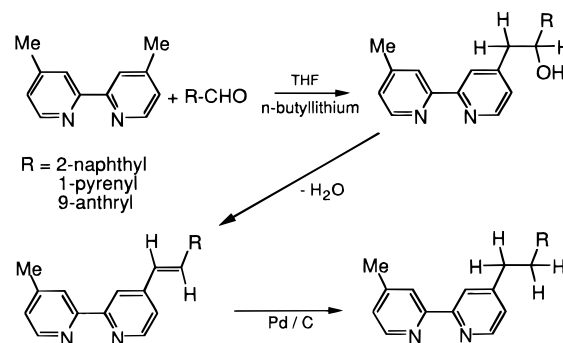
Inasmuch as structural versatility is the key to these systems, we have been particularly interested in controlling the excited-state properties of $\text{Ru}(\text{bpy})_3^{2+}$ using pendant aromatic chromophores tethered by a short flexible link to one or more of the bipyridine ligands.⁵ In earlier work we described the room-temperature singlet and triplet energy-transfer processes involved in a series of bichromophores comprising [Ru] linked to naphthalene, pyrene, and anthracene groups, where [Ru] is $\text{Ru}(\text{bpy})_2(4\text{-methyl-4'-(2-ethyl)-2,2'-bipyridine})$. In the present work we extend our earlier studies to include a full description of the excited-state properties of these bichromophores at room temperature and at 77 K. Also, in the case of [Ru]-anthracene, which is photosensitive, the photodegradation products have been identified.

2. Experimental Section

The photophysics and photochemistry of the ligands and their precursors are interesting in their own right, and their synthesis and spectroscopy will be described elsewhere. The ligand precursors were prepared according to Scheme 1, and their purity was confirmed by melting point, ^1H and ^{13}C NMR, and microanalysis. The complexes were synthesized according to previous methods.⁶

Absorption spectra were measured using a Cary-5E spectrophotometer, and the steady-state emission and excitation spectra

SCHEME 1



were measured using a Perkin-Elmer MPF-44 fluorimeter. In the emission and transient absorption experiments a variety of excitation sources was used in order to selectively excite specific chromophores in the complexes. Excitation sources included a Molelectron nitrogen laser (337 nm), a Lambda-Physik LPX-100 excimer laser (248 and 351 nm), and an excimer-pumped Molelectron DL-II dye laser using coumarin 460 dye (460 nm). Transient absorption spectra were obtained using a PARC OMA III detection system. The pump beam was focused to a line in a 1 cm sample cell using a cylindrical lens. The collimated output of a 150 W Xe lamp was used to probe the excited sample, and the transmitted light was delivered to the OMA via a fiber optic bundle. A beamsplitter in front of the fiber optic bundle redirected some of the analyzing light to a Bausch and Lomb monochromator/photomultiplier detection system for kinetic analysis of the transient absorption signals. The signals were detected with an EMI 9658b photomultiplier and digitized using a Tektronix 460a digital oscilloscope.

3. Results

The room-temperature absorption spectra of the bichromophores in methanol are shown in Figure 1. Also shown in Figure 1a,b are the emission and corrected excitation spectra for [Ru]-naphthalene and [Ru]-pyrene; no emission was ob-

[⊗] Abstract published in *Advance ACS Abstracts*, June 15, 1997.

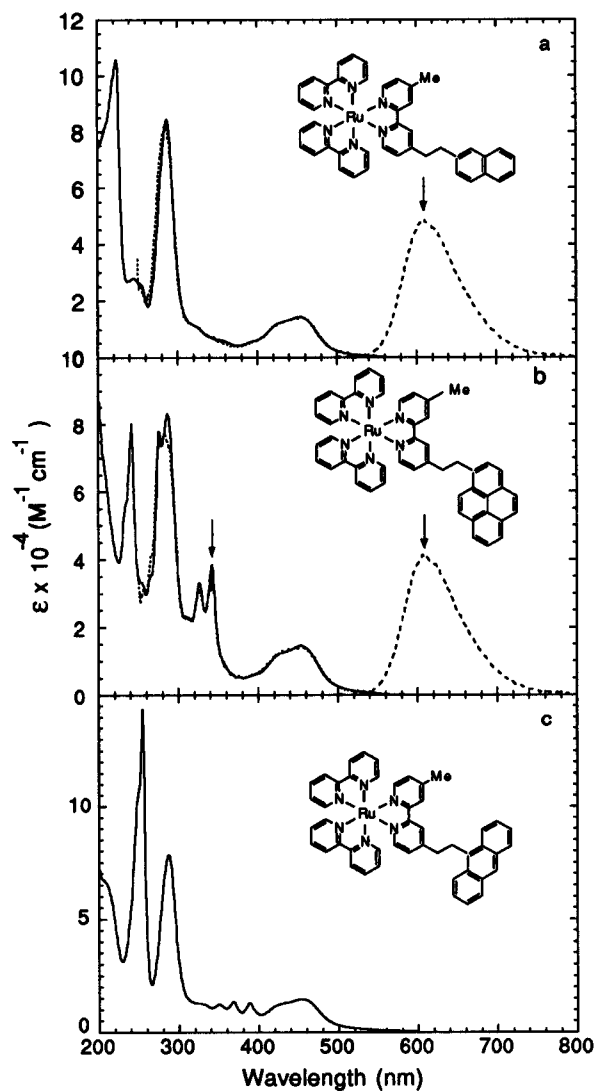


Figure 1. Absorption (—), emission (---) and corrected excitation (···) spectra of (a) [Ru]-naphthalene, (b) [Ru]-pyrene, and (c) [Ru]-anthracene in degassed methanol at room temperature. For the [Ru]-naphthalene emission spectrum ($\lambda_{\text{exc}} = 460$ nm), whereas for [Ru]-pyrene ($\lambda_{\text{exc}} = 337$ nm). Excitation and observation wavelengths are indicated by arrows.

served from the [Ru]-anthracene complex. Nor was there evidence of locally excited fluorescence from any of the pendant aromatic chromophores following direct excitation into their absorption bands. Typical transient absorption spectra of the bichromophores measured in degassed methanol at room temperature are shown in Figure 2. The spectra were recorded at different delays after the laser pulse and in each case the intensity-normalized early- and late-gated spectra were indistinguishable from each other. Identical spectra were also obtained when the excitation wavelength was varied (e.g., $\lambda_{\text{exc}} = 248, 337, 350,$ and 460 nm). The time-resolved emission spectra of [Ru]-pyrene at room temperature and 77 K are shown in Figure 3. Also included as inserts in Figure 3 are the semilog plots of the emission intensity versus time. The excitation wavelength in each case was 337 nm. [Ru]-naphthalene and [Ru]-pyrene were found to be photostable under the experimental conditions used here, and there was no measurable change to the excitation spectrum even after prolonged exposure to actinic light. In contrast, [Ru]-anthracene was found to be extremely photosensitive. The time-resolved emission spectra for [Ru]-anthracene at 77 K are shown in Figure 4a–c. They were recorded from a sample that had been exposed to actinic

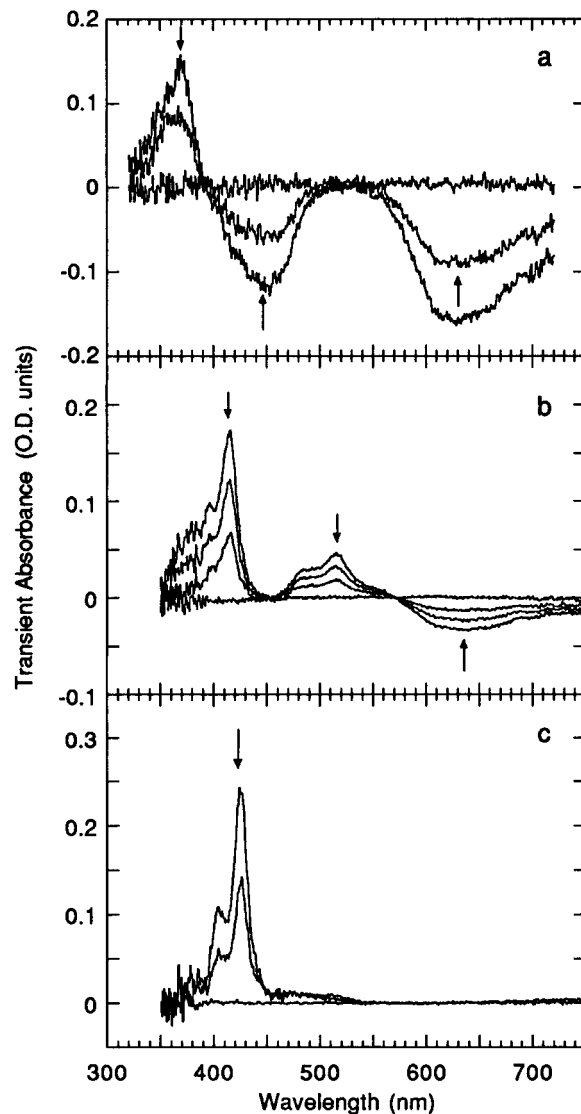


Figure 2. Time-resolved transient absorption spectra measured in methanol at room temperature. Arrows indicate increasing time delay after laser pulse. (a) [Ru]-naphthalene; gate width 100 ns; delay 50 ns, 500 ns, and 2.5 μs . (b) [Ru]-pyrene; gate width 200 ns; delay 50 ns, 1.2 μs , and 3.2 μs . (c) [Ru]-anthracene; gate width 200 ns; delay 50 ns, 7.25 μs , and 500 μs .

light at room temperature prior to freezing to 77 K. The spectra were recorded at various delays after the 337 nm laser pulse, respectively, and show the emission arising from the photodegradation products. Figure 4d shows the low-temperature emission spectrum of a freshly prepared solution of [Ru]-anthracene that had previously been maintained in the dark. The increase in the [Ru]-anthracene photodegradation product and the concomitant decrease in the anthracene phosphorescence as a function of irradiation time are shown in Figure 5. In these experiments the emission spectra at 77 K ($\lambda_{\text{exc}} = 337$ nm) were measured following successive irradiations at room temperature using an excimer laser ($\lambda_{\text{exc}} = 351$ nm). The various spectroscopic properties of the complexes and their component chromophores are collected in Table 1.

4. Discussion

In most cases the absorption spectra of the pendant aromatic groups are well separated from those of the [Ru] chromophore and as a result the assignments of the transitions in the [Ru]-aryl complexes are relatively straightforward. Compared to their parent compounds (Table 1) there are some slight shifts and

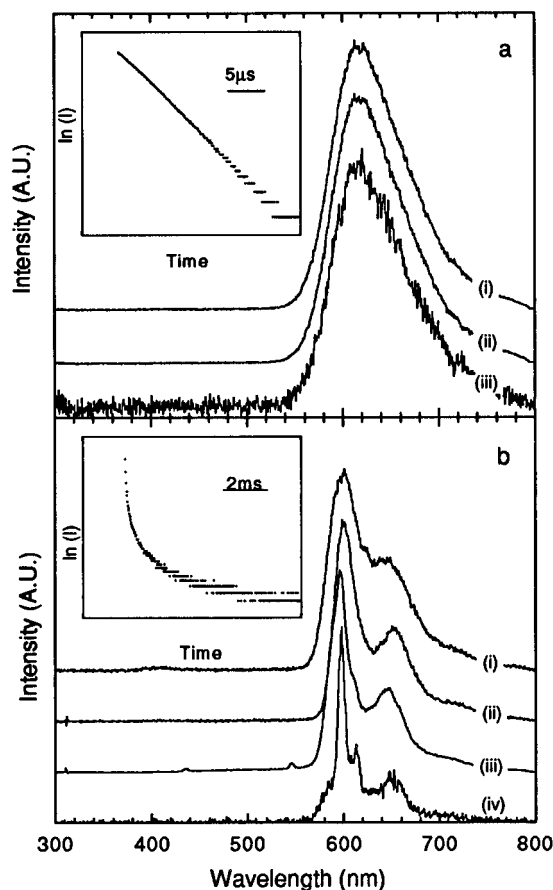


Figure 3. Time-resolved emission spectra ($\lambda_{\text{exc}} = 337$ nm) for [Ru]-pyrene in (a) methanol at room temperature measured with the following delay/gate width settings: (i) 1.6 $\mu\text{s}/100$ ns; (ii) 11 $\mu\text{s}/1$ μs ; and (iii) 25 $\mu\text{s}/1$ μs ; (b) a methanol:ethanol glass at 77 K measured with the following delay/gate width settings: (i) 1.6 $\mu\text{s}/100$ ns; (ii) 100 $\mu\text{s}/10$ μs ; (iii) 10 ms/1 ms; (iv) 500 ms/10 ms. The insets show a plot of the $\ln(\text{intensity})$ of the emission at 620 nm versus time.

broadening of the vibronic bands of the pendant aromatic groups; however, despite the proximity of the participating chromophores and the flexibility of the intervening link, we conclude from the absorption spectra that there is little if any ground-state interaction between the tethered chromophores.

4.1. [Ru]-naphthalene. For [Ru]-naphthalene (Figure 1a) the absorption spectrum in the region 240–500 nm is dominated by transitions that are due to the [Ru] chromophore. In this region photoselection of either the $^1\text{L}_a$ or $^1\text{L}_b$ bands of the pendant naphthalene chromophore is difficult due to the overlapping contributions of the MLCT state at 250 nm and the intense ligand-centered $\pi-\pi^*$ states of bipyridine at 287 nm. In contrast, between 200 and 240 nm the absorption spectrum is dominated by the intense naphthalene $^1\text{B}_b$ transition ($\lambda = 225$ nm, $\epsilon = 106\,000$ M^{-1} cm^{-1}) which is slightly red-shifted with respect to the 2-methylnaphthalene chromophore.

The emission spectra of [Ru]-naphthalene and $\text{Ru}(\text{bpy})_3^{2+}$ are similar. They feature a broad, structureless emission with an intensity maximum at 610 nm and an emission lifetime of 810 ns. The emission quantum yield for [Ru]-Naphthalene is slightly higher than that for $\text{Ru}(\text{bpy})_3^{2+}$, and for both complexes the emission spectrum is independent of the excitation wavelength. No evidence was found for any naphthalene fluorescence following its direct excitation at 225 nm. The time-resolved emission spectra of [Ru]-naphthalene and $\text{Ru}(\text{bpy})_3^{2+}$ in a methanol:ethanol glass at 77 K are also very similar. They show a slight blue-shift of the emission maximum and an increase in the resolution in the vibronic structure compared to the room-

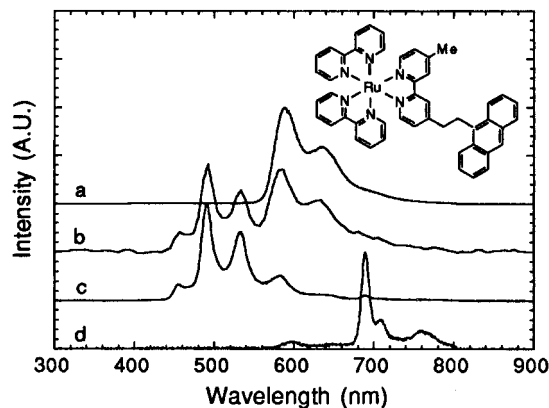


Figure 4. Emission spectra ($\lambda_{\text{exc}} = 337$ nm) in a methanol:ethanol glass at 77 K of a [Ru]-anthracene solution that had previously been exposed to actinic light at room temperature measured using the following delay/gate width settings: (a) 1 $\mu\text{s}/1$ μs ; (b) 40 $\mu\text{s}/10$ μs ; (c) 100 $\mu\text{s}/10$ ms. (d) Emission spectrum ($\lambda_{\text{exc}} = 460$ nm) of a freshly prepared solution of [Ru]-anthracene in a methanol:ethanol glass at 77 K measured 100 μs after the laser pulse and using a gate width of 10 ms.

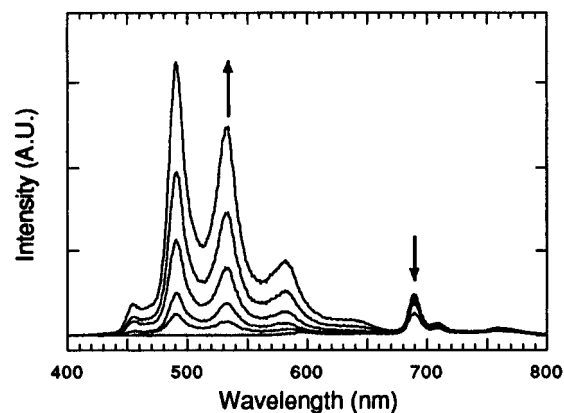


Figure 5. Emission spectra of [Ru]-anthracene at 77 K ($\lambda_{\text{exc}} = 337$ nm) as a function of exposure to actinic light at room temperature.

temperature spectra. Again, neither fluorescence nor phosphorescence was observed from the naphthalene chromophore following laser excitation (248 nm) at 77 K. The lack of naphthalene fluorescence both at room temperature and 77 K indicates efficient quenching of the naphthalene singlet state. Since the fluorescence lifetime for 2-methylnaphthalene in 95% ethanol is 47 ns,⁷ the intramolecular quenching of the naphthalene fluorescence in [Ru]-naphthalene must be substantially faster ($k_q \geq 10^{10}$ s^{-1}). There are two possible quenching mechanisms. The first involves singlet–singlet energy transfer from naphthalene to [Ru] followed by intersystem crossing within the [Ru] manifold to give the $^3\text{MLCT}$ state (pathway α , Scheme 2); the second mechanism involves intersystem crossing within the naphthalene manifold to produce the naphthalene triplet state which is then followed by triplet–triplet energy transfer to the $^3\text{MLCT}$ state (pathway 1- α , Scheme 2).

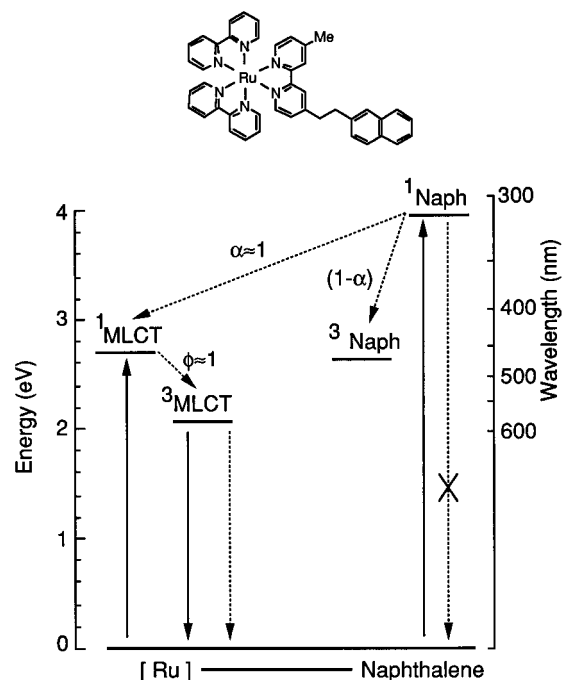
Identification of the actual mechanism is difficult; however, the former is more likely for the following reasons. There is no evidence of any naphthalene phosphorescence from the time-resolved emission data. Furthermore, examination of Figure 2a reveals that the transient absorption spectra of [Ru]-naphthalene are composed of transitions that can be assigned to the [Ru] chromophore alone, namely: (i) a strong absorption at 370 nm due to $^3[\text{Ru}]$, (ii) bleaching of the ground state of [Ru] at 450 nm, and (iii) emission from the [Ru] chromophore at 630 nm. At no time after the laser pulse ($\lambda_{\text{exc}} = 248$ nm) is there any evidence for the naphthalene triplet state. In contrast,

TABLE 1: Photophysical Data for the Bichromophores and Their Components in Methanol

	λ (nm)	ϵ ($M^{-1} \text{ cm}^{-1}$)	state	component chromophore	ϕ_{em} 293 K	τ_{em} (μs)		T-T absorption 293 K	
						293 K	77 K		
Ru(bipy) $_3^{2+}$	453	14 600	MLCT		0.045 ^a	0.720	5.19	370 nm	0.72 μs
	287	84 400	$\pi-\pi^*$						
2-Me naphthalene	319 ^b	^b 530	1L_b		0.16 ^c	^c 0.047		420 nm ^c	
	275	4 800	1L_a						
	224	81 000	1B_b						
1-Me pyrene	342 ^b	^b 50 000	1L_a			^d 0.229		415 nm ^c	
	274	63 000	1B_b					515 nm	
	241	100 000	1B_a						
9-Me anthracene	386 ^b	^b 9 700	1L_a		0.29 ^c	^c 0.005		425 nm ^c	
	256	20 500	1B_b						
[Ru]-naphthalene	460	13 900	MLCT	[Ru]	0.052	0.81	5.21	450 nm	0.80 μs
	287	84 500	$\pi-\pi^*$	[Ru]				370 nm	0.80 μs
	225	105 700	1B_b	naphthalene					
[Ru]-pyrene	460	14 000	MLCT	[Ru]	0.044	5.23	$\left\{ \begin{array}{l} 1130 \text{ 14\%} \\ 7090 \text{ 22\%} \\ 70000 \text{ 64\%} \end{array} \right.$	415 nm	5.24 μs
	343	38 500	1L_a	pyrene					
	287	83 200	$\pi-\pi^*$	[Ry]					
	276	77 900	1B_b	pyrene					
	242	80 200	1B_a	pyrene					
[Ru]-anthracene	460	14 000	MLCT	[Ru]	<0.001			425 nm	350 μs
	390	12 900	1L_a	anthracene					
	287	78 400	$\pi-\pi^*$	[Ru]					
	255	143 600	1B_b	anthracene					

^a Reference 15. ^b Reference 13. ^c Reference 7. ^d Reference 14.

SCHEME 2



an intense triplet-triplet absorption ($\lambda_{\text{max}} = 415 \text{ nm}$, $\epsilon = 25\,000 \text{ L mol}^{-1} \text{ cm}^{-1}$)⁸ was observed for 2-methylnaphthalene using similar excitation conditions. The alternative quenching mechanism ($1-\alpha$) would require a greatly enhanced rate of intersystem crossing within the naphthalene chromophore. It is unlikely even with the proximity of the heavy ruthenium atom that the spin-orbit coupling within the naphthalene chromophore would be increased sufficiently to quench quantitatively the naphthalene excited singlet state. Furthermore, any naphthalene triplet states thus formed would then have to undergo fast intramolecular triplet-triplet energy transfer to the [Ru] chromophore. Quenching mechanism α , therefore, is the more likely due to the absence of any direct evidence for a naphthalene triplet state and the unfavorable spin-orbit considerations necessary for mechanism ($1-\alpha$).

The photophysical properties of the emitting $^3\text{MLCT}$ state of [Ru]-naphthalene and $\text{Ru}(\text{bpy})_3^{2+}$ are similar. Thus, in this particular bichromophore the pendant arene behaves as an efficient light harvesting element for the [Ru] center and the efficiency of energy transfer is close to unity since neither singlet nor triplet naphthalene states are observed spectroscopically.

4.2. [Ru]-pyrene. Absorption by the pyrene chromophore in [Ru]-pyrene occurs as three vibronic progressions with origins at 343 nm (1L_a), 276 nm (1B_b), and 242 nm (1B_a). There is very little shift of these transitions relative to 1-methylpyrene and the highest and lowest energy transitions are well separated from the [Ru] transitions allowing good photoselection in this bichromophore. The 1B_b transition, on the other hand, is obscured by the overlapping contributions from the ligand-centered $\pi-\pi^*$ transitions at 285 nm. The absorption spectrum of [Ru]-pyrene and the corrected excitation spectrum monitored at 610 nm are indistinguishable with peaks attributable to the pyrene chromophore clearly visible in the excitation spectrum at 342, 277, and 242 nm (Figure 1b).

Photoexcitation of the [Ru] chromophore at 460 nm gives rise to a broad, structureless emission that is spectrally indistinguishable from that of the parent $\text{Ru}(\text{bpy})_3^{2+}$ complex. However, the decay of the emission from [Ru]-pyrene has a lifetime of 5.23 μs compared with a lifetime of 720 ns for $\text{Ru}(\text{bpy})_3^{2+}$. This is the longest excited-state lifetime yet observed for a ruthenium trisbipyridyl complex.⁹ Similarly, excitation of [Ru]-pyrene at 337 nm gives rise to the long-lived $^3\text{MLCT}$ emission and there is no evidence of any locally excited pyrene emission despite the fact that at this wavelength absorption by the pyrene chromophore accounts for at least 76% of the total light absorbed by the complex. Clearly, an efficient quenching mechanism is also deactivating the pyrene singlet state. The same fluorescence quenching mechanisms identified for [Ru]-naphthalene are also possible in [Ru]-pyrene. Unfortunately, attempts to resolve the rise time of the $^3\text{MLCT}$ emission at 77 K following excitation of the pyrene chromophore at 337 nm were unsuccessful, and so the rise times must be faster than the time resolution of the equipment used here (10 ns). Nor could we observe any rise time for the pyrene triplet-triplet absorption

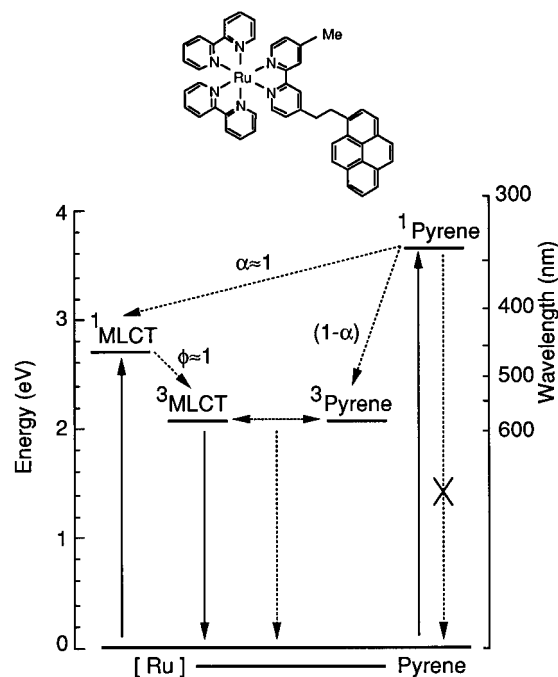
at 410 nm following direct excitation of the [Ru] chromophore at 460 nm. In contrast, a rise time of 7.2 ns was measured for the pyrene triplet–triplet absorption spectrum following excitation into the MLCT state of the phenanthroline-substituted complex.⁹ In this case an identical, fast component was also observed in the emission decay at 600 nm. The linking group in this complex was substantially longer ($-\text{CH}_2-\text{CH}_2-\text{CH}_2-\text{CO}-\text{NH}-$) than the ethane link used in the present work and it is possible that the greater distance between the donor and acceptor groups in their system slowed the intramolecular triplet energy-transfer sufficiently for them to resolve the fast relaxation from the initial, nonequilibrium state.

Time-resolved emission spectra of [Ru]-pyrene excited at 337 nm are shown in Figure 3a. Also included as an insert is a semilog plot of the emission intensity versus time. The intensity-normalized early- and late-gated emission spectra are exactly superimposable, indicating there is no change in the emitting species with time. In contrast, the time-resolved emission spectra for the [Ru]-pyrene complex at 77 K show a very different type of behavior, Figure 3b. The spectrum measured at 1 μs after the laser pulse is dominated by a [Ru]-type emission, ($\lambda_{\text{em}}^{\text{max}} = 601 \text{ nm}$, fwhm = 38 nm). At longer times (up to 10 ms after the laser pulse) the spectra undergo a progressive blue-shift of the emission maximum with a concomitant increase in the resolution of the vibronic structure. Finally, at very long times after the laser pulse (up to 750 ms) the emission spectrum consists of a combination of two distinct emitting species. A more intense, highly resolved spectrum ($\lambda_{\text{em}}^{\text{max}} = 597 \text{ nm}$, fwhm = 10 nm, with a shoulder at 612 nm and a second peak at $\approx 646 \text{ nm}$) superimposed on a less intense, broad spectrum. The former is due to phosphorescence from the pyrene chromophore, while the latter spectrum is identical in shape to the early-gated spectrum, i.e., emission from the [Ru]-centered $^3\text{MLCT}$ state. Therefore, even at delay times of up to 1 s after the laser pulse there is still evidence of residual $^3\text{MLCT}$ emission from [Ru]-pyrene at 77 K. The time evolution of the spectral changes are reflected in the decay profile monitored at 590 nm which is shown as an inset in Figure 3b. The decay is nonexponential and can be adequately fit only by a sum of three exponentials with lifetimes and relative contributions of 1.15 ms (15%), 7.10 ms (20%), and 70 ms (65%), respectively. The emission decays measured at the peak of the pyrene phosphorescence (597 nm) and at the blue edge of the $^3\text{MLCT}$ emission (580 nm) are identical, and so the pyrene triplet state can be thought of as providing a long-lived “reservoir” supplying energy to the emitting $^3\text{MLCT}$ state of the [Ru]-pyrene bichromophore.

The transient absorption spectrum of [Ru]-pyrene at room temperature is characterized by a strong absorption at 410 nm and a weaker one at 515 nm that can be assigned to the triplet–triplet absorption of 1-methylpyrene (Figure 2b). As in the case of [Ru]-naphthalene, emission from [Ru]-pyrene is observed as a negative-going signal at 620 nm. However, in contrast to [Ru]-naphthalene there is no significant bleaching of the transient absorption spectrum in the region 400–500 nm, indicating most of the excitation energy is localized on the pyrene chromophore. Finally, the intensity-normalized early- and late-gated transient absorption spectra are identical with each other over the entire wavelength range, a further indication of the rapid equilibrium between the excited-state species.

The lowest energy triplet states for 1-methylpyrene and $\text{Ru}(\text{bpy})_3^{2+}$ are isoenergetic. Since internal conversion between the two chromophores in [Ru]-pyrene is fast relative to their respective deactivation pathways, the kinetic behavior of the $^3\text{MLCT}$ emission is strongly influenced by the long-lived pyrene

SCHEME 3



triplet state. As a result the decay of the $^3\text{MLCT}$ emission at 610 nm is identical with the decay of the pyrene triplet–triplet absorption monitored at 410 nm (Table 1). The relevant photophysical processes for [Ru]-pyrene are summarized in Scheme 3.

Due to the proximity of the two chromophores and the energetics of the triplet states, efficient energy redistribution occurs between the two chromophores of [Ru]-pyrene. The radiative decay is exclusively via the [Ru] moiety since its radiative rate of $7.7 \times 10^4 \text{ s}^{-1}$ is much greater than the radiative decay rate from the pyrene triplet state at room temperature, $1.25 \times 10^{-2} \text{ s}^{-1}$.¹⁰

The partitioning of the excitation energy between $^3\text{pyrene}$ and $^3\text{MLCT}$ can be determined by examining the $^3\text{MLCT}$ emission at time zero (I_0) following laser excitation at 460 nm of solutions of [Ru]-pyrene and $\text{Ru}(\text{bpy})_3^{2+}$ optically matched at the excitation wavelength. In this case, identical populations of $^3\text{MLCT}$ excited states are formed immediately following dye-laser excitation. However, in the case of [Ru]-pyrene the $^3\text{MLCT}$ state is quickly depopulated by intramolecular energy transfer to the nearby pyrene triplet state, thus lowering the emission intensity. Assuming the radiative and nonradiative rates for the $^3\text{MLCT}$ states in both complexes are similar, analysis of such decay data show that 82% of excited [Ru]-pyrene complexes have the initial excitation localized on the pyrene chromophore. The remaining 18% have the excitation energy localized in the [Ru] $^3\text{MLCT}$ state. A similar estimation for the excited-state partition ratio can be determined from the photophysical data listed in Table 1. In this case I_0 is calculated from the ratio of the emission quantum yield and the emission lifetime. This analysis yields a partition ratio of 85:15 for the excitation localized on the pyrene and [Ru] chromophores, respectively. These ratios are confirmed qualitatively by the results of the transient absorption spectra which show intense absorptions due to the pyrene triplet state with little bleaching of the [Ru] $^3\text{MLCT}$ state at 450 nm. The value for the partition ratio can be used to calculate the relative rates of triplet energy transfer between the two chromophores in [Ru]-pyrene using eq 1,⁹ where k_f is the rate of energy transfer from $^3\text{MLCT}$ to $^3\text{pyrene}$ and k_r is the reverse process. Taking a mean value of

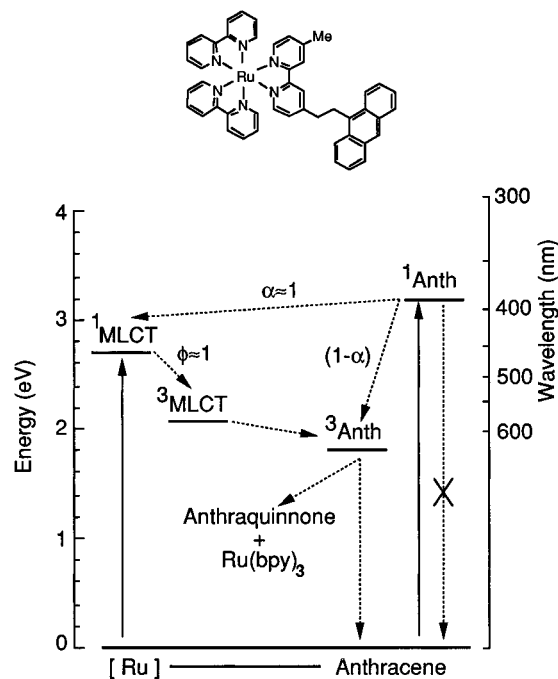
$$K_{\text{eq}} = \frac{k_f}{k_r} = \frac{[\text{Ru}(\text{bpy})_3]^*_0}{[\text{Ru}(\text{bpy})_3]^*_{\text{equil}}} - 1 \quad (1)$$

15% for $[\text{Ru}(\text{bpy})_3]^*_{\text{equil}}$, then $k_f = 5.7 k_r$. In the related phenanthroline-pyrene system k_f was found to be 18 times faster than k_r .⁹

4.3. [Ru]-anthracene. The 1L_a (340–400 nm) and 1B_b (254 nm) transitions of the anthracene chromophore are clearly visible in the absorption spectrum of [Ru]-anthracene (Figure 1c) allowing good photoselectivity in this bichromophore. In contrast to the other bichromophores, there is no evidence of emission from either the $^3\text{MLCT}$ state following excitation at 460 nm nor of anthracene fluorescence following direct excitation of the anthracene chromophore at 390 nm. Furthermore, the transient absorption spectra of [Ru]-anthracene (Figure 2c) show no features that can be assigned to the [Ru] chromophore even at very early times after the laser pulse. Instead, only an intense absorption which is due to the anthracene triplet state is observed at 425 nm. This transient absorption decays exponentially ($\tau = 350 \mu\text{s}$) in degassed methanol. The efficient production of the anthracene triplet state combined with its long lifetime results in very efficient triplet-triplet quenching (annihilation) even at low concentrations (10^{-5} M). This accounts for the erroneous half-life reported earlier for this complex.⁵

Despite being nonluminescent, prolonged exposure of [Ru]-anthracene to light ($\lambda_{\text{exc}} \leq 460$ nm) results in an emission developing at 610 nm the intensity of which increases with irradiation time. This emission is spectrally and kinetically indistinguishable from that of the parent $\text{Ru}(\text{bpy})_3^{2+}$ chromophore, and its appearance is accompanied by a decrease in the intensity of the anthracene 1L_a absorption in [Ru]-anthracene. This suggests that the emission arises from a system in which the anthracene chromophore has undergone photodegradation to products that are unable to quench the [Ru] $^3\text{MLCT}$ state. Similar results have been reported for a structurally related complex.¹¹ It is well-known that triplet anthracene readily undergoes photooxidation across the 9,10 position to form the endo-peroxide which can rearrange to form the relatively nonfluorescent anthraquinone chromophore. For [Ru]-anthracene oxidative degradation by this pathway could then lead to the aryl group becoming detached from the [Ru] center. This degradation pathway for [Ru]-anthracene is confirmed by the low-temperature emission spectra (Figure 4). The spectra shown in Figure 4a–c were recorded from a sample of [Ru]-anthracene that had been exposed to actinic light at room temperature prior to freezing to 77 K. Figure 4a was recorded 1 μs after the 337 nm laser pulse and is characteristic of the $\text{Ru}(\text{bpy})_3^{2+}$ complex at this temperature. Figures 4b and 4c were recorded 40 and 100 μs after the 337 nm laser pulse and show the emergence of the characteristic anthraquinone phosphorescence at 456, 490, 533, and 581 nm.¹² Finally, Figure 4d shows the low-temperature emission spectrum of a freshly prepared solution of [Ru]-anthracene that had been previously kept in the dark. The spectrum was recorded 100 μs after the laser pulse ($\lambda_{\text{exc}} = 460$ nm) and is dominated by peaks at 690 and 760 nm and a shoulder at 709 nm, all of which are characteristic of anthracene phosphorescence. A weak emission from the $\text{Ru}(\text{bpy})_3^{2+}$ moiety at 600 nm is probably due to the buildup of a small amount of $\text{Ru}(\text{bpy})_3^{2+}$ photolysis products. The increase in the photodegradation product as a function of irradiation time is shown in Figure 5. In these experiments the emission spectra at 77 K were measured following successive irradiations at room temperature ($\lambda_{\text{exc}} = 351$ nm). The anthraquinone triplet is more energetic than the anthracene triplet, but more importantly it

SCHEME 4



lies 5200 cm^{-1} above the [Ru]-centered $^3\text{MLCT}$ state. Photodegradation of the anthracene chromophore, therefore, results in a system in which the $^3\text{MLCT}$ state is no longer quenched, and consequently emission from the $^3\text{MLCT}$ state returns. The relevant photophysical processes for [Ru]-anthracene are summarized in Scheme 4.

Photoexcitation of either chromophore of the [Ru]-anthracene complex results in the formation of $^3\text{anthracene}$ with unit quantum yield. In this case the anthracene triplet state acts as an efficient light-harvesting sink for [Ru]-anthracene, and both the rate of singlet-singlet energy transfer from excited anthracene to the $^1\text{MLCT}$ state and triplet-triplet energy transfer from $^3\text{MLCT}$ back to the anthracene chromophore are rapid.

5. Conclusions

The photophysics and photochemistry of a series bichromophores of the type [Ru]-aryl have been investigated, and we have shown that the localization of the initial excitation energy can be controlled in a systematic manner. For [Ru]-naphthalene the initial energy is localized on the [Ru]-centered $^3\text{MLCT}$ state ($E = 2.12 \text{ eV}$, $\tau = 0.81 \mu\text{s}$). In contrast, for [Ru]-anthracene the initial energy is localized on the triplet state of the pendant aromatic chromophore ($E = 1.8 \text{ eV}$, $\tau = 350 \mu\text{s}$). In the case of [Ru]-pyrene the excitation energy is delocalized over both chromophores with $\approx 85\%$ localized on the pyrene chromophore and $\approx 15\%$ on the [Ru]-centered $^3\text{MLCT}$ state ($E = 2.12 \text{ eV}$, $\tau = 5.23 \mu\text{s}$). Furthermore, the participating triplet states are in rapid equilibrium even at 77 K. Generally speaking, good photoselection of the individual chromophores is possible. Emission and transient absorption experiments show that the excited singlet states of the pendant aromatic groups are quantitatively quenched by intramolecular energy transfer to the [Ru] component. The extent of triplet-triplet energy transfer between the $^3\text{MLCT}$ state and the pendant aromatic triplet states is dependent on the relative triplet energy levels. The lifetimes of these bichromophores reflect the multiplicity of the lowest excited states. Thus [Ru]-naphthalene has the shortest excited-state lifetime (0.810 μs) in keeping with its MLCT parentage, whereas [Ru]-anthracene has the longest (350 μs) reflecting its almost pure triplet character. The lifetime of [Ru]-pyrene is

intermediate between these due to the excited-state equilibrium between the two portions of the bichromophore.

References and Notes

- (1) (a) Balzani, V.; Juris, A.; Venturi, M.; Campagna, S.; Serroni, S. *Chem. Rev.*, **1996**, *96*, 759. (b) Hanan, G. S.; Arana, C. R.; Lehn, J.-M.; Fenske, D. *Angew. Chem., Int. Ed. Engl.* **1995**, *34*, 1122. (c) Balzani, V.; Moggi, L.; Scandola, F. In *Supramolecular Photochemistry*; Balzani, V., Ed.; Reidel: Dordrecht, The Netherlands, 1987, 1. (d) De Cola, L.; Balzani, V.; Barigelletti, F.; Flamigni, L.; Belser, P.; Bernhard, S. *J. R. Netherlands Chem. Soc.* **1995**, *114*, 534.
- (2) (a) Arkin, M. R.; Stemp, E. D. A.; Turro, C.; Turro, N. J.; Barton, J. K. *J. Am. Chem. Soc.* **1996**, *118*, 2267. (b) Kamat, P. V.; Bedja, I.; Hotchandani, S.; Patterson, L. K. *J. Phys. Chem.* **1996**, *100*, 4900. (c) Ford, W. E.; Wessels, J. M.; Rodgers, M. A. *J. Langmuir* **1996**, *12*, 3449.
- (3) (a) Sauvage, J.-P.; Collin, J.-P.; Chambron, J.-C.; Guillerez, S.; Coudret, C.; Balzani, V.; Barigelletti, F.; De Cola, L.; Flamigni, L. *Chem. Rev.* **1994**, *94*, 993. (b) Grosshenny, V.; Harriman, A.; Hissler, M.; Ziessel, R. *J. Chem. Soc., Faraday Trans.* **1996**, *92*, 2223. (c) Belser, P.; Dux, R.; Baak, M.; De Cola, L.; Balzani, V. *Angew. Chem., Int. Ed. Engl.* **1995**, *34*, 595.
- (4) (a) Indelli, M. T.; Scandola, F.; Collin, J. P.; Sauvage, J. P.; Sour, A. *Inorg. Chem.* **1996**, *35*, 303. (b) Yoshimura, A.; Nozaki, K.; Ikeda, N.; Ohno, T. *J. Phys. Chem.* **1996**, *100*, 1630. (c) Opperman, K. A.; Mecklenburg, S. L.; Meyer, T. J. *Inorg. Chem.* **1994**, *33*, 5295. (b) Jones Jr, W. E.; Bignozzi, C. A.; Chen, P.; Meyer, T. J. *Inorg. Chem.* **1993**, *32*, 1167.
- (5) Wilson, G. J.; Sasse, W. H. F.; Mau, A. W.-H. *Chem. Phys. Lett.* **1996**, *250*, 583.
- (6) Johansen, O.; Kowala, C.; Mau, A. W.-H.; Sasse, W. H. F. *Aust. J. Chem.* **1979**, *32*, 1453.
- (7) Birks, J. B.; *Photophysics of Aromatic Molecules*; Wiley-Interscience: 1970; p 127.
- (8) Carmichael, I.; Hug, G. L. *J. Phys. Chem. Ref. Data.* **1986**, *15*, 1.
- (9) A similar phenomenon has been observed for a related system in which a pyrene chromophore was covalently attached to the 1,10-phenanthroline ligand of a Ru(bipy)₂(phen) complex. In this case the lifetime of the emitting state was increased to 11.2 μs. Ford, W. E.; Rodgers, M. A. *J. Phys. Chem.* **1992**, *96*, 2917.
- (10) Langelaar, J.; Rettschnick, R. P. H.; Hoijtink, G. J. *J. Chem. Phys.* **1971**, *54*, 1.
- (11) Weinheimer, C.; Choi, Y.; Caldwell, T.; Gresham, P.; Olmsted III, J. *J. Photochem. Photobiol. A: Chem.* **1994**, *78*, 119.
- (12) Parker, C. A. *Photoluminescence of Solutions*; Elsevier: The Netherlands, 1968; p 462.
- (13) Friedel, R.; Orchin, M. *Ultraviolet Spectra of Organic Compounds*; J. Wiley and Sons: New York, 1951.
- (14) Wong, A. L.; Hunnicutt, M. L.; Harris, J. M. *J. Phys. Chem.* **1991**, *95*, 4489.
- (15) Nakamaru, K. *Bull. Chem. Soc. Jpn.* **1982**, *55*, 1639.